Soil Dynamics and Earthquake Engineering 95 (2017) 9–16

Contents lists available at ScienceDirect

Soil Dynamics and Earthquake Engineering

journal homepage: www.elsevier.com/locate/soildyn

Efficient solution for the diffraction of elastic SH waves by a wedge: Performance of various exact, asymptotic and simplified solutions

Víctor H. Aristizabal[a,b,*], Francisco J. Velez[a,b], Juan D. Jaramillo[a]

[a] Departamento de Ingeniería Civil, Universidad EAFIT, Medellín, Colombia
[b] Facultad de Ingeniería, Universidad Cooperativa de Colombia, Medellín, Colombia

ARTICLE INFO

Keywords:
Elastic waves
Diffracted waves
Analytic solution
Performance of solutions
Geometrical theory of diffraction
Wedge diffraction

ABSTRACT

The diffraction of horizontally polarized shear waves by a semi-infinite wedge in frequency and time domains is studied. In particular, this work focus on the performance of different solutions, including the classical contributions from Macdonald, Sommerfeld and Kouyoumjian & Pathak. In addition, two fully analytical, simplified solutions are proposed using arguments from the so-called geometrical theory of diffraction. The main advantage of the two proposed solutions is the fact that the resulting solutions can be scaled to problems with arbitrary and complex geometries. Moreover, it is found that one of the proposed new solutions is highly efficient in terms of accuracy and computational speed as compared to alternative formulations (approximately 1000 times faster than the Macdonald and Kouyoumjian & Pathak solutions), thus, this important characteristic renders this solution ideal for implementation in GPUs (Graphics Processor Units) for multiscale modeling applications.

1. Introduction

The scattering of elastic waves by arbitrarily shaped surfaces that generate geometric effects is important in many practical applications, such as soil exploration when searching for natural sources, geotechnical applications, rock mechanics and earthquake engineering. For a comprehensive literature review on the diffraction problem for wedges and its applications the reader may consult the work by Jaramillo et al. [1].

In this work, the performance of different solutions for a wedge-shaped surface with incident, horizontally polarized, shear (SH) waves is studied. The problem of elastic wave propagation in a wedge is relevant from the viewpoint of the geometrical theory of diffraction [2,3] because it allows for scaling to more complex problems from the application of basic problems called "canonical problems" [1]; these ideas have been widely used in other areas due to its scalability and relative ease in numerical implementations and its sufficient accuracy for engineering applications [4,5].

This paper is organized as follows. In Section 2, the geometric field is briefly presented. In Section 3, the Macdonald exact solution in series expansion in terms of Bessel functions for the total field of a wedge is given. In Section 4, the Sommerfeld asymptotic solution, or the Keller solution, is described, which is a non-uniform solution at high frequency ($k_s r \gg 1$) because it is not valid near the reflection and transmission boundaries. In Sections 5, 6 and 7, the solution of Kouyoumjian & Pathak and simplified solutions 1 and 2 are presented, which are uniform solutions. The Sommerfeld (asymptotic), Kouyoumjian & Pathak, and simplified solutions 1 and 2 are based on the ideas of the geometrical theory of diffraction. Finally, a comparative study of accuracy and computational performance of these solutions is performed.

2. Geometric solution

First, a geometric description of the two-dimensional problem of a plane harmonic SH wave falling on a clamped or traction-free wedge is provided in this section. Fig. 1 shows the geometric solution, where the discontinuity of the displacement field at the incident and reflection boundaries can be observed.

Fig. 1 shows the three wedge-shaped regions defined by the half-plane and the directions of the reflected and transmitted rays:

$$\text{Reflection region:} 0 \le \phi \le \pi - \phi_0$$

$$\text{Transmission region:} \pi - \phi_0 \le \phi \le \pi + \phi_0 \quad \text{Shadow region:} \pi + \phi_0 \le \phi \le \nu\pi. \tag{1}$$

Now, an incident plane SH wave falling at ϕ_0 is considered. The time factor $e^{i\omega t}$ is assumed and is omitted, and the g superscript

* Corresponding author: Facultad de Ingeniería, Universidad Cooperativa de Colombia, A.A. 50630 Medellín, Colombia.
E-mail addresses: vharisti@yahoo.com (V.H. Aristizabal), fjvelezh@gmail.com (F.J. Velez), jjarami@eafit.edu.co (J.D. Jaramillo).

http://dx.doi.org/10.1016/j.soildyn.2017.01.040
Received 8 January 2016; Received in revised form 31 October 2016; Accepted 26 January 2017
Available online 02 February 2017

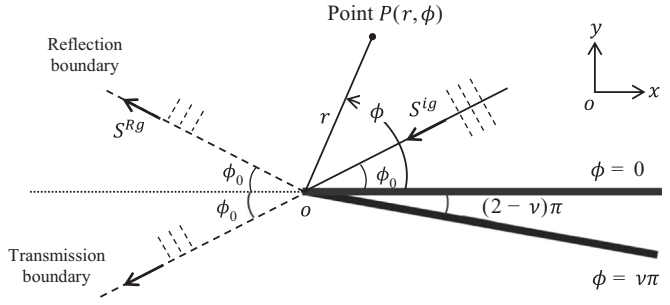

Fig. 1. Geometric displacement field of a plane SH wave falling on a wedge, where r and ϕ are cylindrical coordinates.

indicates the geometric field:

$$S^{ig} = u_0 e^{-i\vec{k}_s^{ig}\bullet\vec{r}}$$

$$= u_0 e^{ik_s(x\cos\phi_0 + y\sin\phi_0)} = u_0 e^{ik_s r\cos(\phi-\phi_0)}, \tag{2}$$

which, after incidence in a plane-discontinuity, generates a reflected plane SH wave:

$$S^{Rg} = u_0 R_{SH} e^{-i\vec{k}_s^{Rg}\bullet\vec{r}}$$

$$= u_0 R_{SH} e^{ik_s(x\cos\phi_0 - y\sin\phi_0)} = u_0 R_{SH} e^{ik_s r\cos(\phi+\phi_0)}, \tag{3}$$

where $k_s = 2\pi/\lambda_s = \omega/c_s = 2\pi f/c_s$ is the wavenumber for secondary waves, ω is the angular frequency, f is the frequency, and c_s and λ_s are the propagation velocity and the wavelength for secondary waves, respectively. The reflection coefficient R_{SH} is

$$R_{SH} = \begin{cases} -1, \text{for a clamped boundary (Dirichlet condition)} \\ 1, \text{for a traction-free boundary (Neumann condition)} \end{cases} \tag{4}$$

Finally, the total geometric solution can be defined as

$$\text{Reflection region: } u^g = S^{ig} + S^{Rg}$$

$$\text{Transmission region: } u^g = S^{Rg} \quad \text{Shadow region: } u^g = 0. \tag{5}$$

3. Macdonald exact solution

Second, the exact solution of Macdonald to the problem of a plane SH wave diffracted by a wedge-shaped medium is given by [6,7]

$$u_{exact}(r,\phi) = S^i + S^R \tag{6}$$

with

$$S^i = \frac{2u_0}{\nu}\sum_{n=0}^{\infty}\epsilon_n e^{i\pi\eta_n/2} J_{\eta_n}(k_s r)\cos[\eta_n(\phi-\phi_0)] \quad S^R = \frac{2u_0 R_{SH}}{\nu}\sum_{n=0}^{\infty}\epsilon_n e^{i\pi\eta_n/2} J_{\eta_n}(k_s r)\cos[\eta_n(\phi+\phi_0)] \tag{7}$$

where $\eta_n = n/\nu$, R_{SH} is the reflection coefficient defined in (4) and

$$\epsilon_n = \begin{cases} \epsilon_0 = \epsilon_1 = \epsilon_2 = \ldots = 1, & \text{for a clamped boundary} \\ \epsilon_0 = 1/2, \quad \epsilon_1 = \epsilon_2 = \ldots = 1, & \text{for a traction-free boundary} \end{cases} \tag{8}$$

Here, it is important to note that the Macdonald series expansion has a very slow convergence for large values of $k_s r$, that is, when $k_s r \gg 1$.

4. Sommerfeld asymptotic solution or Keller solution (non-uniform)

Third, the Sommerfeld asymptotic solution for high frequency [6] (also called the non-uniform solution), which was also achieved by Keller through the geometrical theory of diffraction [2], is given by

$$u_{non}(r,\phi) = S^i_{non} + S^R_{non} \tag{9}$$

where

$$S^i_{non} = u_0 e^{(ik_s r\cos(\phi-\phi_0)} h[\cos(\tfrac{\phi-\phi_0}{2})] + u_0 \frac{e^{(-ik_s r)}}{\sqrt{k_s r}} D^i_{non},$$

$$S^R_{non} = u_0 R_{SH} e^{ik_s r\cos(\phi-\phi_0)} h[\cos(\tfrac{\phi+\phi_0}{2})] + u_0 R_{SH} \frac{e^{-ik_s r}}{\sqrt{k_s r}} D^R_{non}, \tag{10}$$

where $h(X)$, the Heaviside unit-step function, is defined as

$$h(X) = \begin{cases} 1 & \text{if } X \geq 0 \\ 0 & \text{if } X < 0 \end{cases}; \tag{11}$$

and

$$D^i_{non} = \frac{(e^{(-i\pi/4)}\sin(\frac{\pi}{\nu}))}{\nu\sqrt{2\pi}}\left[\frac{1}{\cos\left(\frac{\pi}{\nu}\right) - \cos\left(\frac{\phi-\phi_0}{2}\right)}\right],$$

$$D^R_{non} = \frac{e^{-i\pi/4}\sin\left(\frac{\pi}{\nu}\right)}{\nu\sqrt{2\pi}}\left[\frac{1}{\cos\left(\frac{\pi}{\nu}\right) - \cos\left(\frac{\phi+\phi_0}{2}\right)}\right] \tag{12}$$

are the first-order diffraction coefficients of the Sommerfeld asymptotic solution. This asymptotic solution can also be written and understood as

$$u_{non}(r,\phi) = u^g + u^d_{non} \tag{13}$$

where

$$u^d_{non} = u_0\frac{e^{-ik_s r}}{\sqrt{k_s r}} D^i_{non} + u_0 R_{SH}\frac{e^{-ik_s r}}{\sqrt{k_s r}} D^R_{non} \tag{14}$$

is the diffracted field of the non-uniform solution and

$$u^g = u_0 e^{ik_s r\cos(\phi-\phi_0)} h\left[\cos\left(\frac{\phi-\phi_0}{2}\right)\right] + u_0 R_{SH} e^{ik_s r\cos(\phi+\phi_0)} h\left[\cos\left(\frac{\phi+\phi_0}{2}\right)\right]$$

$$= S^{ig} h\left[\cos\left(\frac{\phi-\phi_0}{2}\right)\right] + S^{Rg} h\left[\cos\left(\frac{\phi+\phi_0}{2}\right)\right] \tag{15}$$

is the same geometric field defined in (5) in compact form, representing the total field. The signs of $\cos(\frac{\phi\pm\phi_0}{2})$ within the regions defined in (1) and (5) are as follows:

$$\text{Reflection región: } u_{som} = S^{ig} + S^{Rg} + u^d_{non};\ \cos\left(\frac{\phi-\phi_0}{2}\right) > 0, \quad \cos\left(\frac{\phi+\phi_0}{2}\right) > 0$$

$$\text{Transmission region: } u_{som} = S^{ig} + u^d_{non};\ \cos\left(\frac{\phi-\phi_0}{2}\right) > 0,$$

$$\cos\left(\frac{\phi+\phi_0}{2}\right) < 0 \quad \text{Shadow region: } u_{som} = u^d_{non};\ \cos\left(\frac{\phi-\phi_0}{2}\right) < 0,\ \cos\left(\frac{\phi+\phi_0}{2}\right) < 0. \tag{16}$$

In Fig. 2, the wavefront pattern of the Sommerfeld asymptotic solution is shown for $0 < \phi_0 < \pi/2$.

5. Kouyoumjian & Pathak solution (uniform)

Fourth, the Kouyoumjian & Pathak solution for high frequency [1,3] (also called the uniform solution) is an improvement of the Sommerfeld asymptotic solution based on the Keller method [2], achieved by proposing diffraction coefficients that remain valid near the reflection and transmission boundaries, where the coefficients in (12) fail. Then, this solution is given by

$$u_{uni}(r,\phi) = u^g + u^d_{uni} \tag{17}$$

where u^g is the same geometric field defined in (15) and

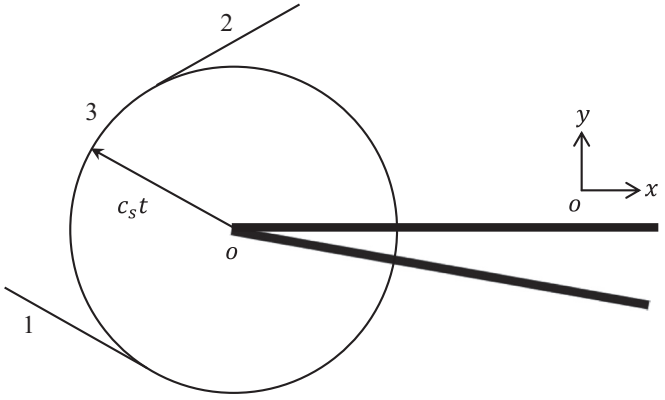

Fig. 2. Wavefront Pattern of the Sommerfeld asymptotic field for a plane SH wave with a wedge, where $1 = S^{ig}h\left[\cos\left(\frac{\phi-\phi_0}{2}\right)\right]$, $2 = S^{Rg}h\left[\cos\left(\frac{\phi+\phi_0}{2}\right)\right]$ and $3 = u^d_{non}$.

$$u^d_{uni}=u_0\frac{e^{-ik_s r}}{\sqrt{k_s r}}D^i_{uni}+u_0 R_{SH}\frac{e^{-ik_s r}}{\sqrt{k_s r}}D^R_{uni} \tag{18}$$

is the diffracted field of the uniform solution.

The diffraction coefficients proposed by Kouyoumjian & Pathak are given by

$$\begin{aligned} D^i_{uni} &= -\frac{e^{-i\pi/4}}{2\nu\sqrt{2\pi}}\left\{\cot\left[\frac{\pi+(\phi-\phi_0)}{2\nu}\right]F[a^+(\phi-\phi_0)]\right. \\ &\quad \left.+\cot\left[\frac{\pi-(\phi-\phi_0)}{2\nu}\right]F[a^-(\phi-\phi_0)]\right\},\ D^R_{uni} \\ &= -\frac{e^{-i\pi/4}}{2\nu\sqrt{2\pi}}\left\{\cot\left[\frac{\pi+(\phi+\phi_0)}{2\nu}\right]F[a^+(\phi+\phi_0)]\right. \\ &\quad \left.+\cot\left[\frac{\pi-(\phi+\phi_0)}{2\nu}\right]F[a^-(\phi+\phi_0)]\right\} \end{aligned} \tag{19}$$

$$a^{\pm}(\beta) = 2k_s L\cos^2\left(\frac{2\nu\pi N^{\pm}-\beta}{2}\right),$$

$$L=\begin{cases} r & for\ incident\ plane\ waves \\ \frac{rr_0}{r+r_0} & for\ incident\ cylindrical\ waves\ of\ radius\ r_0 \end{cases},$$

$$N^+=\begin{cases}0\ if\ \beta\le\nu\pi-\pi\\ 1\ if\ \beta>\nu\pi-\pi\end{cases},\ N^-=\begin{cases}-1\ if\ \beta<\pi-\nu\pi\\ 0\ if\ \pi-\nu\pi\le\beta\le\pi\le+\nu\pi\\ 1\ if\ \beta>\pi+\nu\pi\end{cases}$$

and $F(X)$ is the transition function defined in (20), which involves a Fresnel integral.

$$F(X)=2i\sqrt{X}e^{iX}\int_{\sqrt{X}}^{\infty}e^{-iq^2}dq=2i\sqrt{\frac{X\pi}{2}}e^{iX}\left\{\left[\frac{1}{2}-C\left(\sqrt{\frac{2X}{\pi}}\right)\right]-i\left[\frac{1}{2}-S\left(\sqrt{\frac{2X}{\pi}}\right)\right]\right\} \tag{20}$$

,

where $s(X)$ and $c(X)$ are the Fresnel integrals given by [8–10]

$$\begin{aligned} S(X) &= \int_0^X \sin(\pi q^2/2)dq, \\ C(X) &= \int_0^X \cos(\pi q^2/2)dq. \end{aligned} \tag{21}$$

6. Simplified uniform solution 1

Fifth, a simplified solution is achieved when the solution (17) is taken and the transition function $F(X)$ defined in (20) is changed by an equivalent analytic function based on [11]

$$F_{E1}(X) = 2i\sqrt{X\pi}e^{i(X-\pi/4)}[1/(1-e^{2\sqrt{X\pi}e^{i\pi/4}})+e^{-i(X+\pi/4)}/\sqrt{4\pi X}] \tag{22}$$

7. Simplified uniform solution 2

Sixth, a second simplified solution is achieved in the same manner as in the previous section, where the transition function $F(X)$ in (20) is changed by [11]

$$F_{E2}(X)=2i\sqrt{X\pi}e^{i(X-\pi/4)}\left\{h(-\sqrt{X})+sgn(\sqrt{X})[1-e^{-\sqrt{\pi}|\sqrt{X}|}]\right. \\ \left.\frac{e^{-i\left(X+\frac{\pi}{4}-\frac{\pi}{4}e^{-|\sqrt{X}|}\right)}}{\sqrt{4\pi|X|}}\right\},$$

$\sqrt{X}\ge 0$, then $h(-\sqrt{X})=0$, $sgn(\sqrt{X})=1$ and $|\sqrt{X}|=\sqrt{X}$, so

$$F_{E2}(X) = 2i\sqrt{X\pi}e^{i(X-\pi/4)}[1-e^{-\sqrt{X\pi}}]e^{-i\left(X+\frac{\pi}{4}-\frac{\pi}{4}e^{-\sqrt{X}}\right)}/\sqrt{4\pi X}, \tag{23}$$

Note that the two simplified solutions are completely analytic.

8. Results and discussion

To study the performance of the solutions presented above, including the two proposed simplified solutions, diffraction in a wedge is analyzed. We take a wedge of 300^0 with a free-traction boundary, where $\nu = 300/180 \approx 1.6667$, on which plane harmonic SH waves fall at $\phi_0=80^0$, as shown in Fig. 3.

8.1. Frequency domain analysis

In Fig. 4, the Macdonald, Sommerfeld asymptotic, Kouyoumjian & Pathak, and simplified uniform solutions 1 and 2 are shown in frequency domain, based on Eqs. (6), (13), (17), (22) and (23) (see Appendix for the Matlab code). For the Macdonald solution, 4000 terms are used in the calculations. All solutions were in agreement, except for the Sommerfeld asymptotic solution at low frequencies ($k_s r<10$) and near the reflection and transmission boundaries.

In Fig. 5, the absolute magnitude and phase errors, $\Delta M = |Mag(u_{exact})-Mag(u_i)|$ and $\Delta P = |Ph(u_{exact})-Ph(u_i)|$, with respect to the Macdonald solution are shown, where u_i is either the Sommerfeld asymptotic, Kouyoumjian & Pathak or simplified uniform solutions 1 and 2. Furthermore, in Fig. 5 can also be observed that the error decreases as $k_s r$ increases. Fig. 4 and 5 show that the Sommerfeld asymptotic solution exhibits large errors at low frequencies ($k_s r < 10$) and near the reflection and transmission boundaries.

The computation times for the different solutions on an Intel Xeon

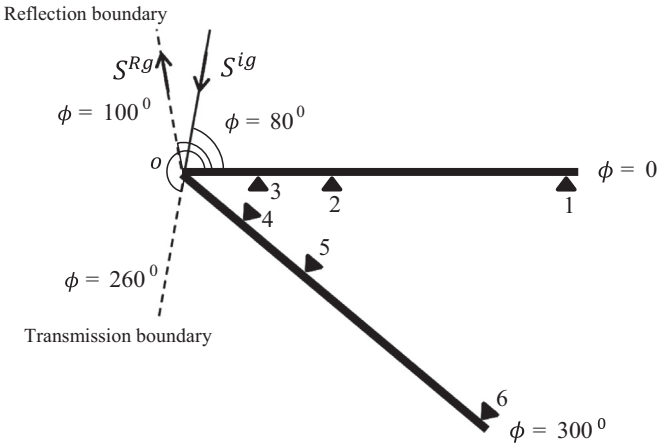

Fig. 3. Sketch of the geometric displacement field of a plane SH wave falling at 80^0 on a wedge of 300^0. The triangles represent the measuring stations for r values: 0.1, 1 and $10km$, on both faces of the wedge.

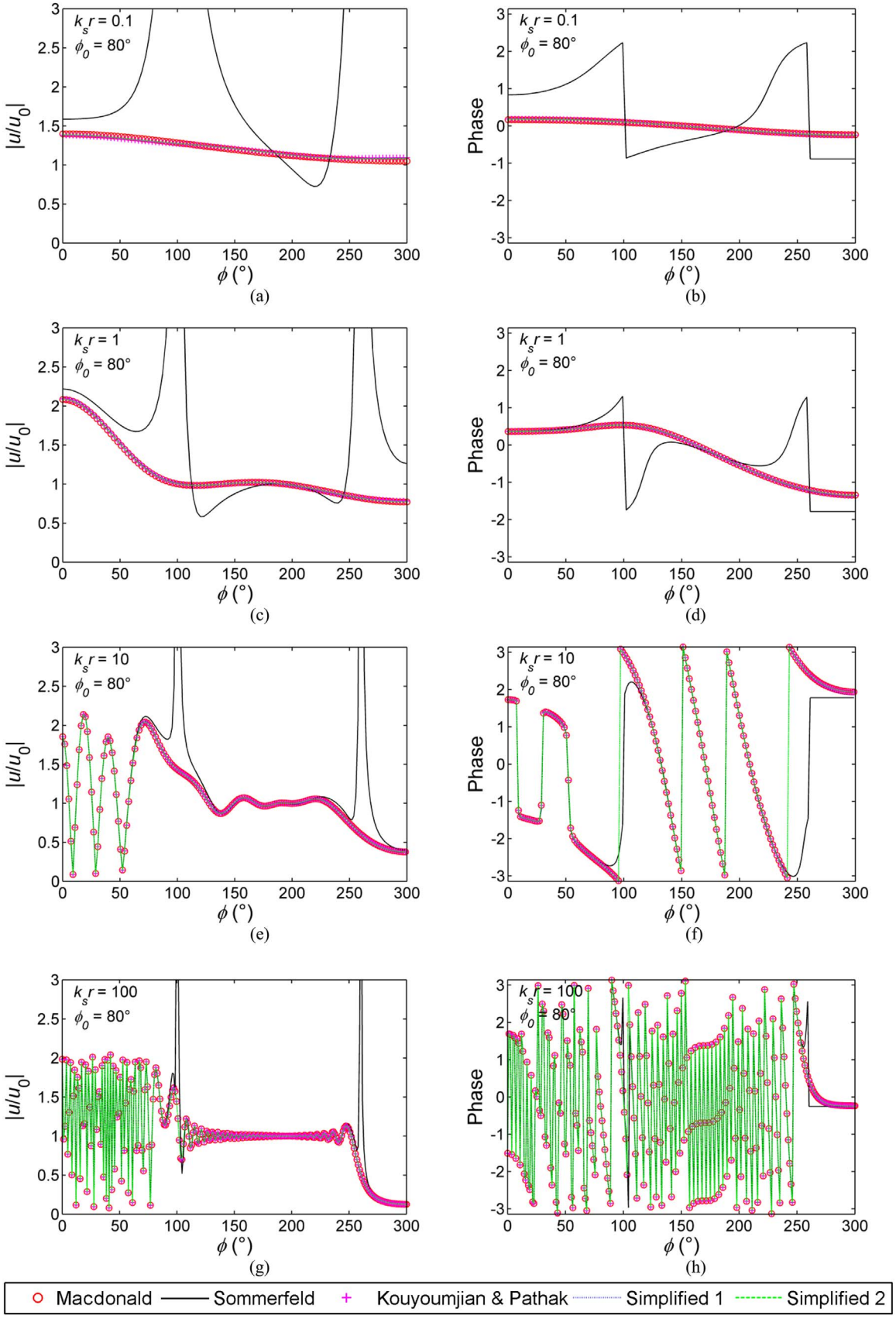

Fig. 4. Magnitude and phase for diffraction in a wedge computed with several solutions for $k_s r$ values: 0.1, 1, 10 and 100.

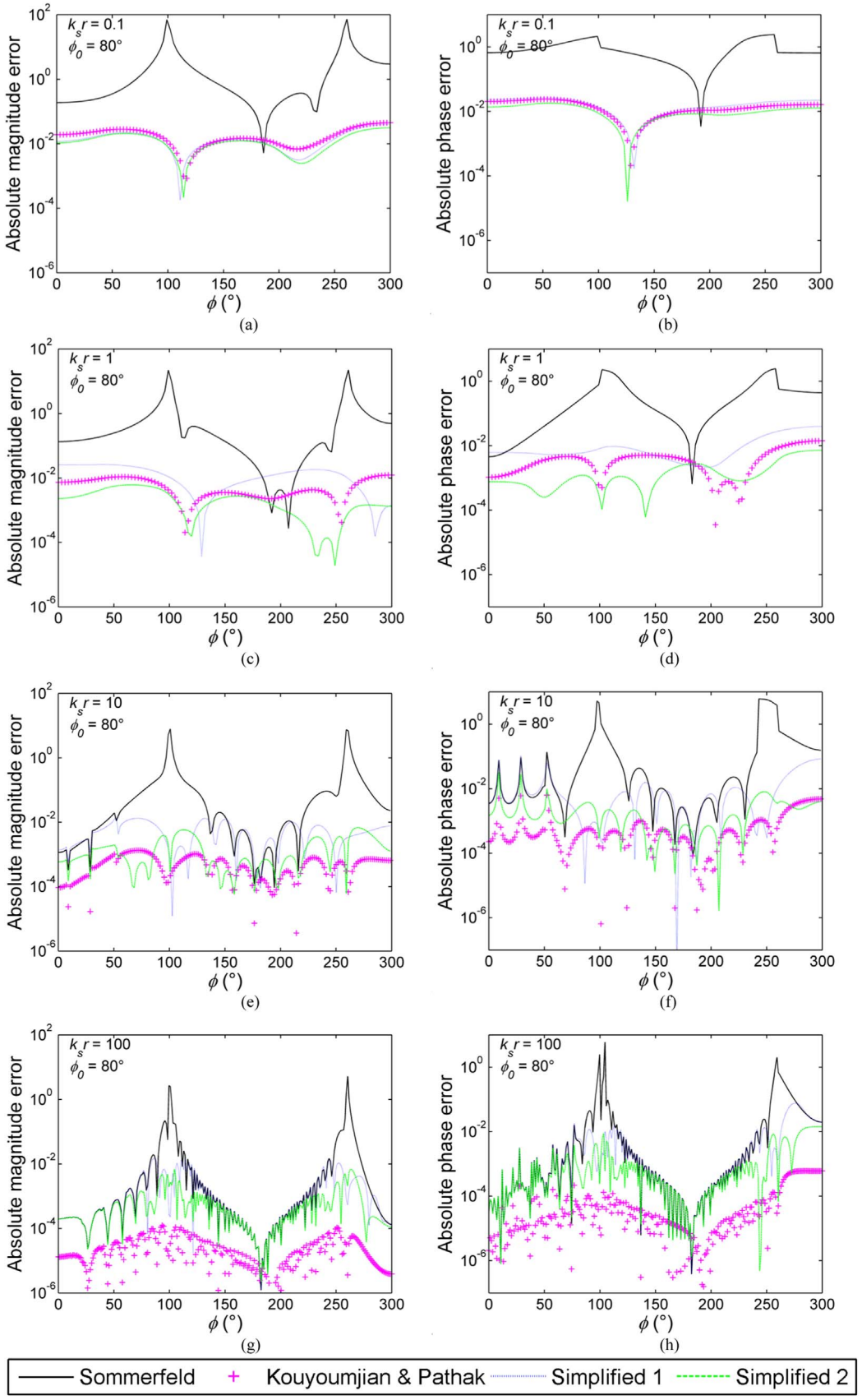

Fig. 5. The absolute errors of the magnitude and phase with respect to the Macdonald solution are computed for $k_s r$ equal to 0.1, 1, 10 and 100. The vertical axis is presented on a logarithmic scale.

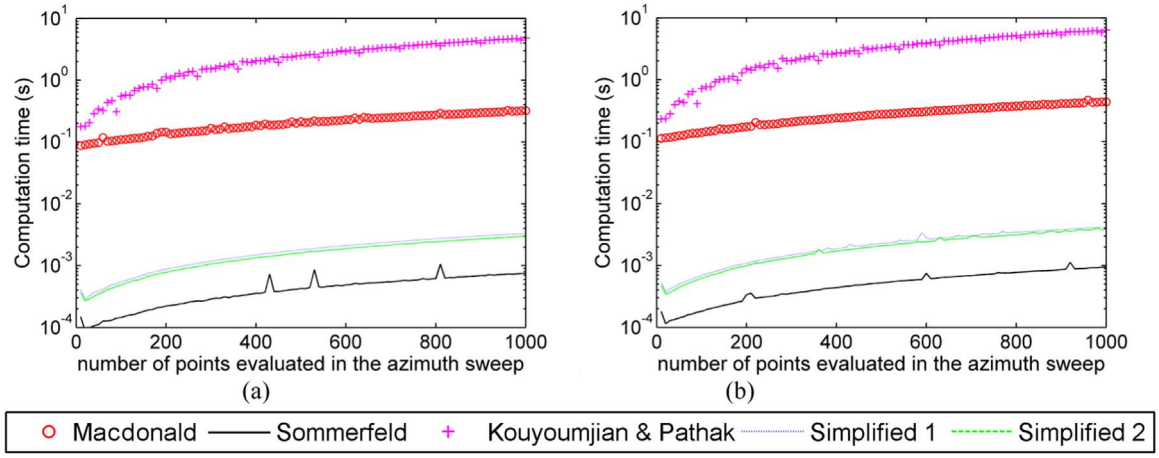

Fig. 6. Computation times for $k_s r = 1$ (a) on an Intel Xeon and (b) on a laptop Intel i3. The vertical axis is presented on a logarithmic scale.

Table 1
Computation times in seconds for $k_s r = 1$.

Solution	Number of points evaluated in the azimuth sweep					
	On a laptop Intel i3, 2.13 GHz, 4 GB RAM			On an Intel Xeon, 2.4 GHz, 64 GB RAM		
	10	100	1000	10	100	1000
Macdonald	0.410356	0.441830	0.759497	0.087734	0.108409	0.316030
Sommerfeld	0.000334	0.000422	0.001250	0.000085	0.000152	0.000725
Kouyoumjian	0.077536	0.643727	7.636763	0.189848	0.548843	4.734227
Simplified 1	0.000471	0.000837	0.004496	0.000264	0.000562	0.003318
Simplified 2	0.000431	0.000762	0.004142	0.000235	0.000499	0.002933

and on a laptop Intel i3 are shown in Fig. 6 and Table 1. In Table 1, for the Intel i3 laptop and with 1000 points evaluated in the azimuth sweep, the results for the Macdonald, Sommerfeld, and simplified uniform solutions 1 and 2 are obtained 10, 6109, 1698 and 1844 times faster than the Kouyoumjian & Pathak solution, respectively, which is in agreement with Fig. 6, which shows that the computation time for the Kouyoumjian & Pathak solution is 1 order of magnitude larger than that of the Macdonald solution and 3 orders of magnitude larger than that of the solutions for the Sommerfeld and simplified uniform solutions 1 and 2 in the range studied.

8.2. Time domain analysis

The frequency domain results were used later in order to find the time domain response using a Fourier transformation approach. For that purpose, a Ricker pulse is taken as

$$R(t)=\{2[\pi f_c (t-t_0)]^2-1\}\, e^{-[\pi f_c (t-t_0)]^2}, \tag{24}$$

where f_c is the central frequency of the pulse and t_0 is the time parameter used to define the star of the active phase. The Fourier transform of the pulse is

$$\Re(\omega)=\int_{-\infty}^{\infty} R(t)e^{-i\omega t}dt=\frac{-2}{f_c\sqrt{\pi}}\left(\frac{\omega}{2\pi f_c}\right)^2 e^{-\left[i\omega t_0+\left(\frac{\omega}{2\pi f_c}\right)^2\right]}. \tag{25}$$

Then, the time history of the wedge displacement field can be achieved from

$$W(t)=\frac{1}{2\pi}\int_{-\infty}^{\infty}\Re(\omega)u_i(\omega)e^{i\omega t}d\omega \tag{26}$$

where $u_i(\omega)$ is either the Macdonald, Sommerfeld asymptotic, Kouyoumjian & Pathak or simplified uniform solutions 1 and 2 defined in Eqs. (6), (13), (17), (22) and (23), respectively.

For the time domain analysis, a f_c=1Hz, a c_s=1kms^{-1} and a t_0=3s for a time window of 20s were taken. In Figs. 7 and 8, the snapshots of the propagation pattern at different times and the time history of the measuring stations on both faces of the wedge for all solutions described in this work are shown. All solutions are in agreement, except for the Sommerfeld asymptotic solution after that the incident front hits on the apex of the wedge near the reflection and transmission boundaries, more precisely, this can be observed in Fig. 8 where the station 4 (see Fig. 3) is the nearest station to the reflection or transmission boundaries.

The computation times for each snapshot with 16,667 points evaluated on the Intel Xeon were: 5277. 713332s for the Macdonald solution, 1. 762731s for the Sommerfeld solution, 5641. 141262s for the Kouyoumjian & Pathak solution, 6.290053s for the simplified solution 1 and 5.711737s for the simplified solution 2. Note that the results for the Sommerfeld, and simplified uniform solutions 1 and 2 are obtained 3200, 897 and 987 times faster than the Kouyoumjian & Pathak solution,

9. Conclusions

In this work, five solutions for the diffraction of elastic SH waves with a wedge are studied, where one solution is exact and, among the other solutions, 1 is non-uniform and 3 are uniform. Numerical comparisons show that the solutions described in Sections 5, 6 and 7 represent the exact solution given by Macdonald in Section 3 with a high degree of accuracy; however, the Sommerfeld solution described in Section 4 is not in total agreement and exhibits large errors at near the reflection and transmission boundaries in both frequency and time domains analysis.

The Sommerfeld (asymptotic), Kouyoumjian & Pathak, and simplified solutions 1 and 2 are based on the geometrical theory of diffraction, which allows more complex problems of arbitrarily shaped

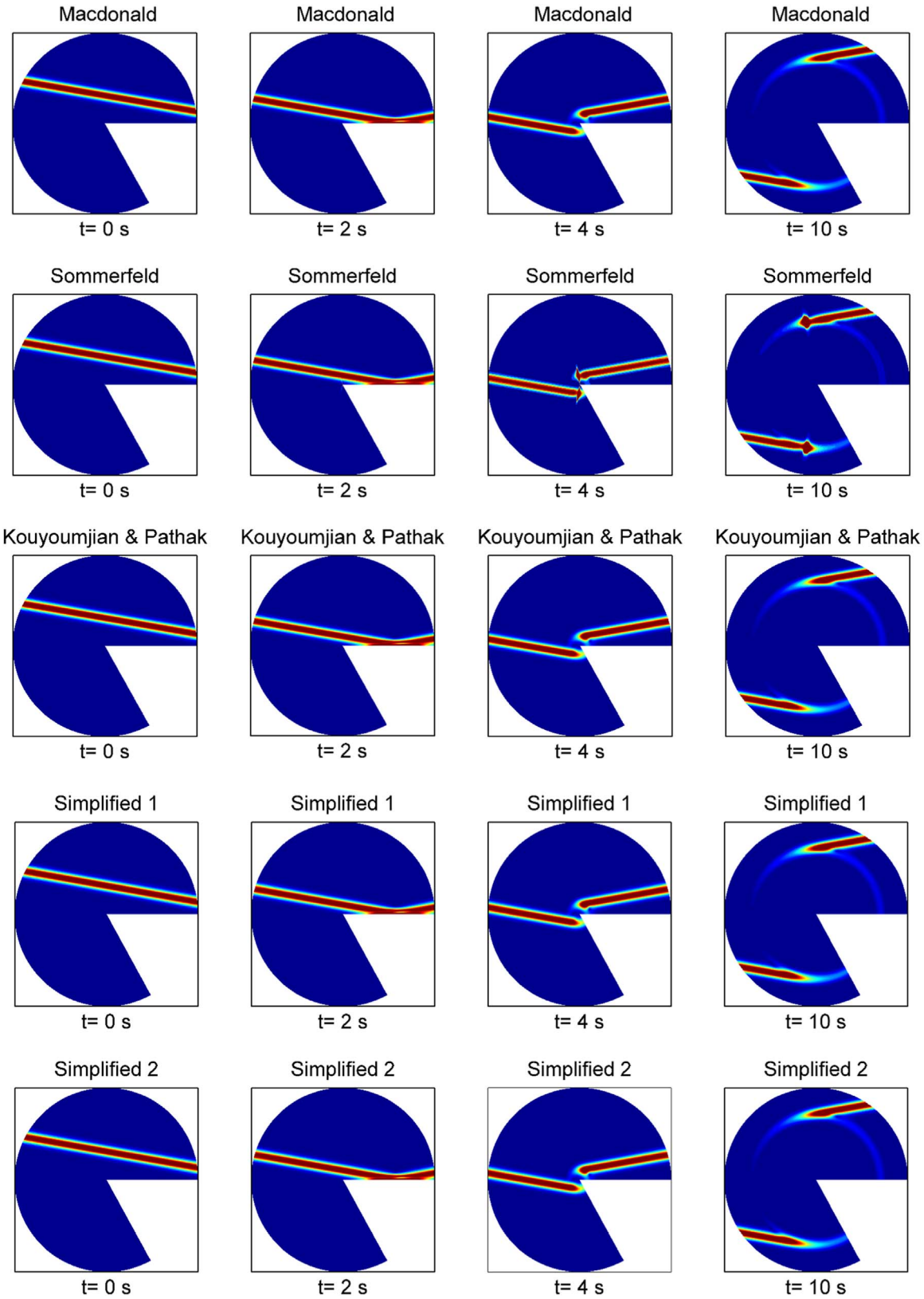

Fig. 7. Snapshots of the propagation patterns for the surface topography shown in Fig. 3 obtained with the Macdonald, Sommerfeld asymptotic, Kouyoumjian & Pathak, simplified solutions 1 and 2. The first column displays the unmodified incident front which is first reflected (column 2) and later diffracted by the singularity at $r = 0$ (column 3 and 4). The snapshots have a radius of $10km$.

surfaces to be studied from the application of a basic problem called a "canonical problem" [1–3], whereas scaling to a more complex problem with the Macdonald solution is not possible.

In regards to performance, the simplified solution 2 is an excellent alternative to the Kouyoumjian & Pathak solution [1,3] because the transition function $F(X)$ presented in the Kouyoumjian & Pathak

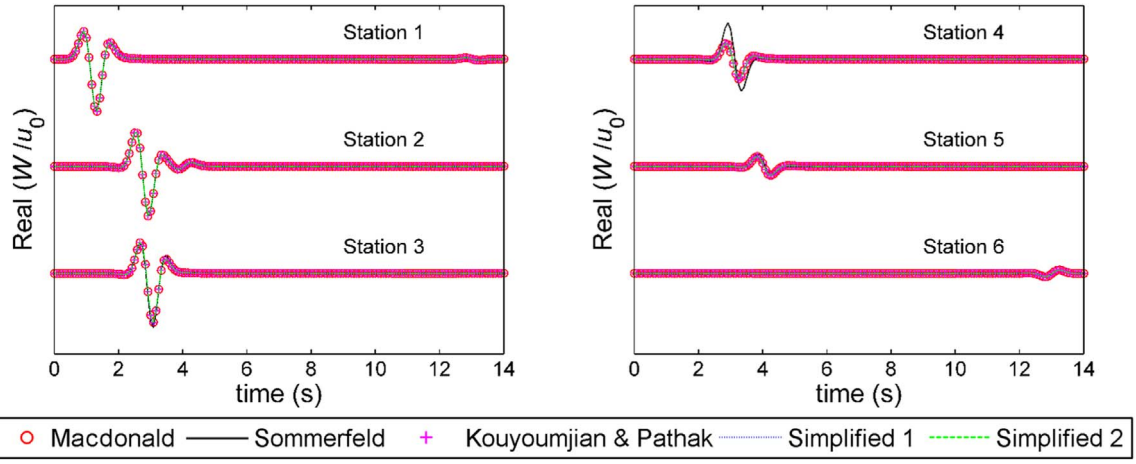

Fig. 8. Time history of displacement for the stations defined in Fig. 3 obtained with the Macdonald, Sommerfeld asymptotic, Kouyoumjian & Pathak, simplified solutions 1 and 2.

solution must be numerically evaluated, thus consuming more memory, and takes approximately 1000 times longer than the simplified solution 2, which is completely analytic. This important characteristic renders the simplified solution 2 ideal for implementation in GPUs (Graphics Processor Units) for multiscale modeling applications. On the other hand, although the Sommerfeld solution seems not to be appropriate under some conditions, worth noting that it is the fastest solution and could be considered when the studies are far away from reflection and transmission boundaries.

Acknowledgments

The authors acknowledge partial support granted by the Administrative Department of Science, Technology and Innovation, Colombai COLCIENCIAS, through the program for national Ph.D. students. V.H. Aristizabal and F.J. Velez acknowledge partial support of the Universidad Cooperativa de Colombia through grants T48-1336 and O42-1044.

Appendix A. Supplementary material

Supplementary data associated with this article can be found in the online version at doi:10.1016/j.soildyn.2017.01.040.

References

[1] Jaramillo J, Gomez J, Saenz M, Vergara J. Analytic approximation to the scattering of antiplane shear waves by free surfaces of arbitrary shape via superposition of incident, reflected and diffracted rays. Geophys J Int 2013;192:1132–43.
[2] Keller JB. Geometrical theory of diffraction. J Opt Soc Am 1962;52:116–30.
[3] Kouyoumjian RG, Pathak PH. Uniform geometrical theory of diffraction for an edge in a perfectly conducting surface. Proc IEEE 1974;62:1448–61.
[4] Kim HS, Kim JS, Kang HJ, Kim BK, Kim SR. Sound diffraction by multiple wedges and thin screens. Appl Acoust 2005;66:1102–19.
[5] Salomons EM. Sound propagation in complex outdoor situations with a non-Refracting atmosphere: model based on analytical solutions for diffraction and reflection. Acta Acust United with Acust 1997;83:436–54.
[6] Ufimstev PY. Wedge diffraction: exact solution and asymptotics. Fundam. Phys. theory Diffr. New Jersey: John Wiley & Sons, Inc; 2007. p. 33–69.
[7] Sánchez-Sesma F. Diffraction of elastic SH waves by wedges. Bull Seismol Soc Am 1985;75:1435–46.
[8] Abramowitz M, Stegun I. Handbook of Mathematical Functions. Washington, D.C.: U.S. Government Printing Office; 1965.
[9] The Mathworks Inc., fresnelS: Mathworks, 2016. ⟨http://www.mathworks.com/help/symbolic/mupad_ref/fresnels.html⟩ [accessed 30.10.16].
[10] The Mathworks Inc., fresnelC: Mathworks, 2016. ⟨http://www.mathworks.com/help/symbolic/mupad_ref/fresnelc.html⟩ [accessed 30.10.16].
[11] Umul YZ. Equivalent functions for the Fresnel integral. Opt Express 2005;13:8469. http://dx.doi.org/10.1364/OPEX.13.008469.